

Synthesis and properties of Zn–Mg heterobimetallic carbamates. Crystal structures of the first reported single source precursors for $Zn_xMg_{1-x}O$ thin films†

Matthew R. Hill,^{*a} Paul Jensen,^b Jennifer J. Russell^c and Robert N. Lamb^d

Received 22nd August 2007, Accepted 12th March 2008

First published as an Advance Article on the web 16th April 2008

DOI: 10.1039/b712952a

The first mixed-metal Zn–Mg carbamates have been synthesised using a novel strategy of co-reaction between zinc and magnesium alkylamido intermediates. The complexes were structurally characterised by single-crystal X-ray diffraction; the nuclearity of these carbamate core subunits was found to vary from tetrameric to octameric with respect to the level of magnesium incorporated. The presence of magnesium in the predominantly zinc carbamate lattice was confirmed by refinement of the site occupancies of the metal atoms during the crystal data analysis, and it was found that displacement of up to 7.8% of zinc sites by magnesium atoms could be achieved before breakdown of the structure. Characterisation of the complexes' physicochemical properties revealed that they were suitable for use as single-source chemical vapour deposition (SSCVD) precursors in the deposition of $Zn_xMg_{1-x}O$ thin films, an emerging material with promising band-gap engineering prospects.

Introduction

There is burgeoning interest in $Zn_xMg_{1-x}O$ thin films, largely because of their tunable band gap and the implications this has for the development of new optoelectronic devices. The similarity in the ionic radii of Zn^{2+} (0.74 Å) and Mg^{2+} (0.71 Å) allows for significant replacement of zinc atoms by magnesium atoms in the ZnO matrix without substantially altering the lattice parameters of the wurtzite crystal. In addition the band gap of MgO (7.8 eV) is much greater than that of ZnO (3.4 eV), so increasing the amount of magnesium in the zinc oxide lattice will result in a proportional widening of the band gap, enabling development of wavelength-tunable optical devices^{1,2} and band-gap engineering.^{2–6} Other reported benefits of this alloying have included an increase in the growth rate of sputtered thin films⁷ and improvements in the degree of film crystallinity.⁸

Single-source chemical vapour deposition (SSCVD) is a simple technique that can be used to derive high-quality thin films without the need for complicated deposition instrumentation. The success of the technique is reliant upon the generation of a precursor that embodies all deposition requirements that are commonly built into deposition equipment. These criteria include: high volatility, clean and efficient decomposition of organic ligands leaving a

clean metal oxide core, synthetic attainability in large quantities, and a temperature 'window' between the onset of sublimation and decomposition. SSCVD has been successfully employed in the past to prepare thin films of materials including ZnS,⁹ ZnO¹⁰ and MgO.^{11,12} In the instance of $Zn_xMg_{1-x}O$, the approach has the added advantage of providing a means of overcoming the difficulties associated with creating an alloyed material through an intimate mixing framework *in situ* at the growth interface, as this level of intimate mixing has already been achieved within the precursor molecule. The technique is highly desirable from a materials creation standpoint, but its utilisation poses a significant challenge to the synthetic chemist due to the stringent precursor requirements.

Development of a precursor molecule that embodies all the attributes described above whilst also being heterobimetallic is a substantial synthetic task. As a consequence, to date there have been no reports of the successful preparation of a $Zn_xMg_{1-x}O$ SSCVD precursor complex. Here we report the development of innovative zinc–magnesium chemistry *en route* to producing heterobimetallic carbamate oligomers and show that these complexes are suitable for use in SSCVD.

Metal carbamate complexes are known to decompose cleanly into the desired metal oxide residues, and we have previously applied some of these complexes in the SSCVD of both ZnO¹⁰ and MgO¹¹ thin films. Metal carbamates generally possess a pre-organised metal oxide core surrounded and protected by volatility-inducing ligands. The known zinc and magnesium carbamate complexes have similar structures, syntheses and properties, and are therefore a solid basis for bimetallic analogues. A limited number of bimetallic carbamate complexes are also known.¹³ The particulars of this chemistry are described herein, demonstrating the points of similarity in zinc and magnesium carbamate chemistry, with a view to interlinking these to generate mixed-metal species.

^aCSIRO Division of Materials Science and Engineering, Private Bag 33, Clayton South MDC, Victoria 3169, Australia. E-mail: matthew.hill@csiro.au

^bCrystal Structure Analysis Facility, School of Chemistry, The University of Sydney, NSW, Australia 2006

^cSchool of Materials Science, University of New South Wales, Anzac Pde Kensington, NSW, Australia 2052

^dSchool of Chemistry, University of Melbourne, Swanston St, Melbourne, VIC, Australia 3010

† CCDC reference numbers 658301 & 658302. For crystallographic data in CIF or other electronic format see DOI: 10.1039/b712952a

Results and discussion

Several possible approaches exist when attempting to synthesise a heterobimetallic SSCVD precursor. Two different approaches are outlined in this work, namely metal-ion scrambling and the production of mixed-metal intermediates. The approaches differ in the timing of the mixing of the species.

Caudle and coworkers reported metal-ion scrambling between isostructural diethylcarbamato hexamers of magnesium and manganese,¹⁴ and cobalt and magnesium.¹⁵ These compounds were prepared simply by mixing the two separate complexes in solution, at elevated temperatures, under pressure in a thick-walled flask to avoid displacement of CO₂ from the complexes. It was shown that this reaction proceeded through the dissociation of one of the hexameric complexes present (manganese or cobalt) into a dimeric state that then reacted with the intact magnesium hexamer to form the heterometallic species. This seemed a promising approach for obtaining a Zn–Mg analogue. In order to apply the metal-ion scrambling approach, the geometries of the species to be combined must first be considered. Several known zinc carbamato complexes with varying alkyl substituents are known to exist. Commonly, these materials arrange themselves with a Zn₄O core (see Fig. 1) surrounded by organic ligands.

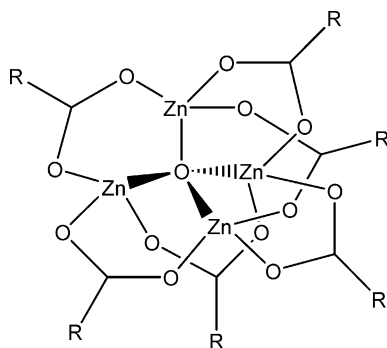


Fig. 1 The Zn₄OR₆ core structure commonly found in zinc carbamates.

The Zn₄O structure has been found in zinc-homoleptic zinc carbamato complexes with R substituents including methyl (**1**),¹⁶ ethyl (**2**),^{10,17,18} butyl (**3**),¹⁹ benzyl (**4**),¹⁹ piperidinyl (**5**)¹⁸ and pyrrolidyl (**6**).¹⁸ These compounds were found to possess differing thermal stabilities and sublimation temperatures, which varied according to the p*K*_a of the amine substituents and the length of the carbon chains.²⁰ Recently, a zinc carbamato complex with an unprecedented geometry was developed in our laboratories. The new octanuclear complex Zn₈O₂(O₂CNⁱPr₂)₁₂ (**7**) consisted of two distorted [Zn₄O]⁶⁺ cores bound together by a web of twelve bridging ⁱPr₂NCO₂⁻ ligands.²¹ This arrangement was isostructural with the few other known octanuclear transition-metal complexes of the ⁱPr₂NCO₂⁻ ligand.^{22–24} The field of zinc carbamato chemistry is dominated by the Zn₄O tetramers **1–6** that can be readily synthesised by various means and form stable, solvent-free structures. The only derivative in this field with a different structure is the octamer **7** which is of interest here because its metal-coordination modes may offer an alternative approach in delivering heterobimetallic complexes.

The structural motifs known within the reported magnesium carbamates are more extensive than the observed zinc moieties. A

class of magnesium carbamates have been reported by Yang and Caudle and their coworkers^{25,26} that have a range of nuclearities depending on the synthesis, ligands and solvents employed. Of note were the hexameric ethyl derivative Mg₆(O₂CNEt₂)₁₂ (**8**), which has previously been reported to be a highly successful SSCVD precursor,^{11,12} its phenyl analogue **9**, and the μ-oxo-bridged isopropyl hexamer Mg₆O(O₂CNⁱPr₂)₁₀ (**10**). Dell'Amico *et al.*²⁷ were able to isolate the ionic salt [Me₂NH₂]₃[Mg₈(CO₃)₂(O₂CNMe₂)₁₅] (**11**) by reaction of MgO with [Me₂NH₂][O₂CNMe₂] under CO₂ atmosphere, and the neutral carbonato-bridged octamer Mg₈(CO₃)₂(O₂CNMe₂)₁₂ (**12**) by exhaustive treatment *in vacuo*. Further variations in nuclearity and coordination modes were found by Tang and co-workers who reported the dimeric cyclohexyl carbamate [Mg₂(O₂CNCy₂)₄][HMPA] (**13**).²⁸ There are a number of structurally distinct magnesium carbamates, possessing nuclearities of 2, 3, 6 and 8 magnesium atoms. However, out of the reported complexes **8–15**, only the hexamers **8** (ethyl), **9** (phenyl) and **10** (isopropyl) exist in the unsolvated state, free of undesirable carbonato residues as required for use in SSCVD applications. This serves to highlight the fact that no isostructural zinc and magnesium carbamates exist. Nevertheless, there are some complexes with similar structures that could potentially still undergo metal-ion scrambling. Studies emulating the reported examples with the Zn–Mg system were undertaken involving reactions of either the zinc isopropyl octamer **7** or the zinc ethyl tetramer **2** with the magnesium ethyl hexamer **8** at elevated temperatures and pressures.

The ethyl derivatives **8** and **2** were mixed in ratios of 25–75% Zn vs. Mg for at least 24 h in heptane at 110°C in thick walled pressure tubes. After slowly cooling the mixture over 24 h a crop of block-shaped crystals formed. Several days later, a second batch of crystals of a different habit was recovered, and single-crystal X-ray diffraction was undertaken on the various crops of crystals. The first batch of crystals had an identical cell volume to the zinc complex **2** and the second batch shared a cell volume equal to the magnesium complex **8**, indicating that only the starting materials were recovered. The occupancies of the metal coordination sites were examined during the structure refinement to provide definitive evidence of the lack of metal-ion scrambling. There was no observable doping of metal sites, indicating a lack of reaction in all instances. The lack of reactivity between the ethyl derivatives **8** and **2** was attributed to the fact that the magnesium complex **8** has hexa-coordinate and penta-coordinate sites, but only tetrahedral coordination modes are present in the zinc derivative **2**. Consequently there are no equivalent metal environments common to **2** and **8** between which metal atoms could migrate.

The zinc isopropyl octamer **7** has two modes of metal coordination, featuring six trigonal bipyramidal and two tetrahedral sites. The co-existence of penta-coordinate sites in both the zinc complex **7** and the magnesium complex **8** would be more likely to be conducive to interchange between these two complexes.

Characterisation of reactions between **7** and **8** revealed a similar inertness, even with the presence of equivalent coordination sites. In contrast, Caudle *et al.*¹⁵ suggested that a mixed Co–Mg complex was formed by trifurcation in solution of a hexameric Co complex into the dimer Co(O₂CNEt₂)₂, which then reacted with the stable magnesium hexamer **8** to yield a mixed-metal product. They also reported that the mixing of isostructural magnesium and

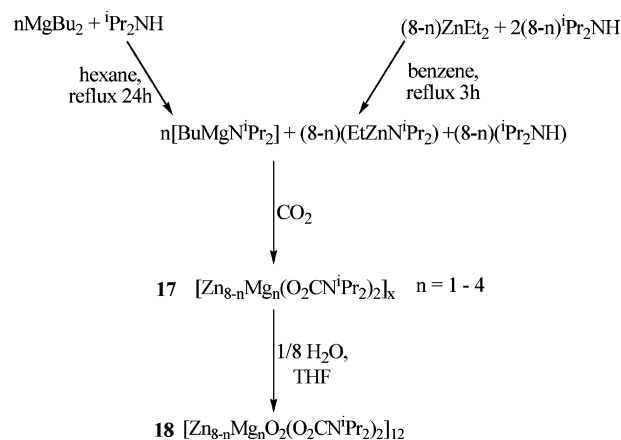
manganese complexes delivered a mixed-metal product that was isostructural to the two starting materials. In the Zn–Mg system, however, no complexes dissociate in solution and there are no known isostructural moieties. Therefore neither of the reported mechanisms could proceed directly in our case, and our results indicate that the reactions do not occur by other means. As a consequence this strategy was not suitable for the generation of a Zn–Mg carbamate complex.

The second approach to obtaining a heterobimetallic complex involves first creating a mixed-metal intermediate. Examples of this approach in the literature are scarce. Ruben and co-workers²⁹ reacted the phenyl oxalamidinato magnesium trimer **14** with excess ZnCl₂ to create a Zn–Mg salt. The complex **14** lost CO₂ in this reaction, and formed the salt [Mg(DMF)₆][Zn₂(L)Cl₄] (**15**) as opposed to a heterobimetallic complex. Bacchi *et al.*¹³ reported the formation of Zn₂Ni₆(μ₄-O)₂(O₂CNⁱPr₂)₁₂ (**16**) as a side product in 3% yield when [Ni(MeCN)₆][ZnCl₄] was exposed to ⁱPr₂NH–CO₂. Within the octameric core, there were tetrahedral and trigonal bipyramidal sites for metal coordination, with the zinc atoms showing a preference for residence in the tetrahedral sites.

Precursors—synthesis and characterisation

Whilst there is scant record of the direct synthesis of heterobimetallic carbamates, descriptions of the formation of carbamate oligomeric complexes in general highlight the coalescence of metal diamido/alkylamido derivatives upon reaction with CO₂ and stoichiometric H₂O as a common pathway, in particular for zinc and magnesium carbamates.^{21,25} These similarities were then exploited through the simultaneous use of zinc and magnesium intermediates to encourage crossover between the two reaction pathways. The goal of this approach was to generate a mixed-metal, oxo-bridged cluster, as illustrated in Scheme 1. The strategy for obtaining the desired complexes *via* mixed-metal intermediates involved the preparation of alkylamido derivatives of zinc¹⁸ and magnesium.^{30,31} Solutions of these two materials were then brought together, and the typical carbamate complexation reaction series carried out. Preliminary observations were useful in gauging the ability to form a complex other than the pure zinc octamer **7**, which would indicate the successful incorporation of Mg. The properties of the compounds were significantly different to **7**, summarised in Table 1.

Two sets of isopropyl groups were observed in ¹H NMR spectra for most of the mixed-metal complexes, in contrast to the pure zinc complex **7** which exhibited only one chemical environment for the isopropyl groups.²¹ The crystal structure of the octamer **7** shows that the molecule is not symmetrical, and therefore two sets of peaks in NMR spectra would be expected. It has been proposed that the octamer is fluxional in solution, alternating to a



Scheme 1 Proposed reaction pathway for Zn–Mg carbamate complexes by co-reaction of amido intermediates.

symmetrical unit such as the known Zn₄O tetramers, accounting for this deviation from expected results.²¹ The magnesium in compounds **19–22** possibly reduced this fluxionality in solution, resulting in the two sets of NMR peaks being observed. The solution properties also varied significantly from the pure zinc complex **7** causing different modes of crystal formation or, in the case of **21** and **22**, an absence. Perhaps the starkest variation in the properties of the proposed mixed-metal derivatives **19–22** from the pure zinc complex **7** was the change in the temperature of sublimation, being 35–45°C lower in the volatile Zn–Mg complexes (*N. B.* the 5 : 3 analogue **21** proved to be involatile).

Single-crystal X-ray diffraction[†] revealed that **19** was tetrameric in structure, in stark contrast to the known Zn octamer **7**. The complex **19** crystallises in the monoclinic space group *P2₁/c* (see Table 2). Whilst being omitted for clarity, the asymmetric unit contains two tetramers and four acetonitrile molecules. One ⁱPr₂NCO₂[−] ligand on each tetramer is disordered over two positions, as witnessed in the ORTEP diagram (Fig. 2, right). All the metal coordination sites within the complex are of tetrahedral geometry. This structure is related to the other known tetrameric zinc carbamates **1–6**. Presumably due to the low doping levels within the complex, no magnesium was detectable in the metal coordination sites of the analysed crystal through refinement of site occupancies. X-Ray Photoelectron Spectroscopy (XPS) lacked the required sensitivity for this direct observation, as the ionisation cross-section for magnesium is relatively small and in any case magnesium was present in quantities less than 1 at%. As a consequence no magnesium photoelectrons were observed during XPS experiments. Although the octamer **7** has been reported as the product of similar reactions when only zinc atoms were present,²¹ it was noted that the complex was fluxional in solution,

Table 1 Properties of products formed from Zn–Mg mixed-precursor solutions.

Zn : Mg starting ratio (identification)	¹ H NMR CH(CH ₃) ₂ /ppm	¹ H NMR CH(CH ₃) ₂ /ppm	Solubility (MeCN)	Solubility (heptane)	Crystallisation solvent	Sublimation temperature/°C (5 × 10 ^{−6} Torr)
8 : 0 (7)	3.91	1.19	Soluble	Slightly soluble	Heptane	205
7 : 1 (19)	2.90, 3.91	1.02, 1.16	Slightly soluble	Soluble	MeCN	160–165
6 : 2 (20)	2.90, 3.91	1.05, 1.15	Totally insoluble	Slightly soluble	Heptane	165–170
5 : 3 (21)	1.14, 2.90	1.04	Slightly soluble	Slightly soluble	None	Involatile
4 : 4 (22)	2.92, 3.91	1.02, 1.16	Soluble	Slightly soluble	None	170

Table 2 Crystal data summary for complexes **19** and **20**†

	19	20
Formula of the refinement model	C ₄₆ H ₉₀ N ₈ O ₁₃ Zn ₄	C _{115.50} H ₂₄₀ N ₁₂ O ₂₆ Zn _{7.38} Mg _{0.62}
Model molecular weight/g mol ⁻¹	1224.74	2710.70
Crystal system	Monoclinic	Rhombohedral
Space group	<i>P</i> 2 ₁ / <i>c</i> (#14)	<i>R</i> $\bar{3}$ (#148)
<i>a</i> /Å	14.355(1)	19.536(3)
<i>b</i> /Å	35.946(2)	19.536(3)
<i>c</i> /Å	24.160(2)	33.566(7)
<i>A</i> /°		90
<i>β</i> /°	99.462(1)	90
<i>γ</i> /°		120
<i>V</i> /Å ³	12297.1(15)	11094(3)
<i>D_c</i> /g cm ⁻³	1.323	1.217
<i>Z</i>	8	3
Crystal size/mm	0.44 × 0.42 × 0.26	0.44 × 0.36 × 0.16
Crystal colour	Colourless	Colourless
Crystal habit	Block	Plate
Temperature/K	150(2)	150(2)
<i>λ</i> (Mo Kα)/Å	0.71073	0.71073
<i>μ</i> (Mo Kα)/mm ⁻¹	1.601	1.337
<i>T</i> (SADABS) _{min,max}	0.590, 0.681	0.593, 0.816
2 θ _{max} /°	56.72	56.70
<i>hkl</i> range	−18–18, −47–46, −32–30	−26–25, −25–25, −44–44
<i>N</i>	123 302	36 154
<i>N</i> _{ind}	29 673 (<i>R</i> _{merge} 0.0478)	5993 (<i>R</i> _{merge} 0.0495)
<i>N</i> _{obs}	20 574 (<i>I</i> > 2 σ (<i>I</i>))	4292 (<i>I</i> > 2 σ (<i>I</i>))
<i>N</i> _{var}	1444	316
Residuals ^a <i>R</i> 1(<i>F</i>), <i>wR</i> 2(<i>F</i> ²)	0.0367, 0.0922 ^a	0.0294, 0.0820 ^b
GoF(all)	1.042	1.090
Residual extrema/e ⁻ Å ⁻³	−0.440, 1.003	−0.328, 0.506

^a $R1 = \sum \|F_o\| - |F_c| / \sum \|F_o\|$ for $F_o > 2\sigma(F_o)$; $wR2 = (\sum w(F_o^2 - F_c^2)^2 / \sum w(F_c^2)^2)^{1/2}$ all reflections. $w = 1/[\sigma^2(F_o^2) + (0.0325P)^2 + 11.5861P]$ where $P = (F_o^2 + 2F_c^2)/3$. ^b $R1 = \sum \|F_o\| - |F_c| / \sum \|F_o\|$ for $F_o > 2\sigma(F_o)$; $wR2 = (\sum w(F_o^2 - F_c^2)^2 / \sum w(F_c^2)^2)^{1/2}$ all reflections. $w = 1/[\sigma^2(F_o^2) + (0.0362P)^2 + 7.4796P]$ where $P = (F_o^2 + 2F_c^2)/3$.

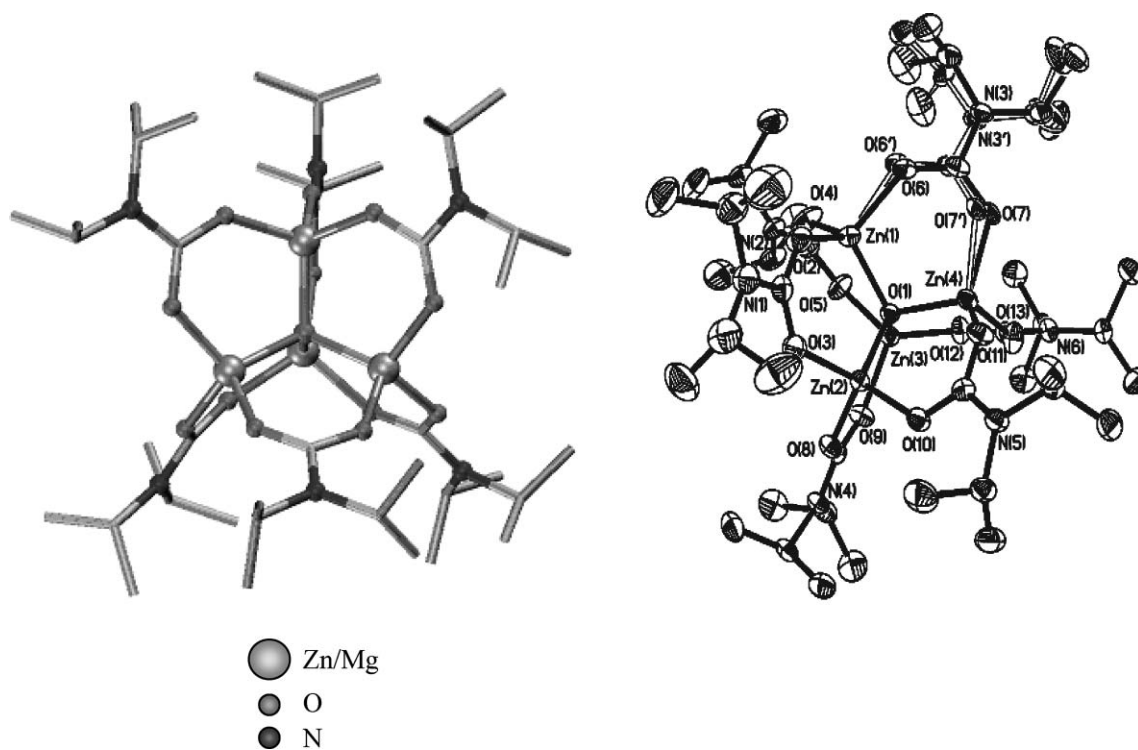
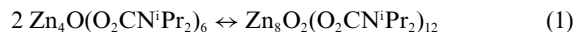


Fig. 2 Graphical representations of **19** as determined by X-ray crystallography.† Hydrogen atoms and acetonitrile solvent molecules have been omitted for clarity. Thermal ellipsoids are drawn at the 50% probability level. (Only one of the two crystallographically unique tetramers is shown.)

as only one set of peaks was observed in NMR spectra. This was indicative of the symmetrical Zn_4O core structure, and suggests that an equilibrium exists, as shown in eqn (1).



The different conformations could then be separately observed by altering the conditions under which crystals were obtained. The NMR spectra of the tetramer **19**, where two sets of peaks are observed, suggests that a similar equilibrium applies for this system, with the formation of an octameric species in solution delivering the two sets of isopropyl groups witnessed in NMR spectra.

As shown in Fig. 3, complex **20** possesses an octameric structure. The core structure of the complex is essentially identical to the geometry observed in the pure zinc octamer **7**, where two Zn_4O tetrahedra are bound together by bridging $^iPr_2NCO_2^-$ ligands that generate six trigonal bipyramidal coordination sites. Complex **20** crystallises in the rhombohedral space group $R\bar{3}$ and contains 4.5 heptane solvent molecules per octamer (see Table 2). The octamer is centred on both inversion and three-fold symmetry elements and thus only 1/6 of the complex is crystallographically unique. Unlike **19** the complexes contain no disorder of the peripheral carbamate ligand groups and pack together to leave a cubic-like network of channels which host extremely disordered heptane solvent. Significantly, magnesium substitution into the metal coordination sites was indicated in this instance by refinement of the metal site occupancies for **20**. These were found to be (Zn : Mg) 0.94 : 0.06 for the tetrahedral site and 0.92 : 0.08 for the trigonal bipyramidal sites. Within the limits of accuracy for the method, this represented a uniform distribution of magnesium atoms across both types of metal coordination sites. Approximately one third of

the magnesium introduced into the reaction flask was successfully introduced into the zinc carbamate complex.

The variations in the crystal structures of **19** and **20** are indicative of the influence of magnesium within the carbamate core. The family of known magnesium carbamates exhibits only five- or six-coordinate magnesium, so its incorporation in significant levels into a mixed Zn–Mg carbamate would be more extensive in a complex with similar sites. Given the equilibrium shown in eqn (1), and the observation of both products under otherwise identical conditions, small changes in the system would be likely to shift the equilibrium. Consequently the presence of magnesium moieties with a preference for five- and six-coordinate states would shift the equilibrium to deliver the octamer. In summary, increased magnesium and its preference for higher coordination number sites shifts the equilibrium described in eqn (1) to the right, delivering the octamer **20**. However, no preference for magnesium location within the five-coordinate sites was found, indicating that although the presence of magnesium may promote the formation of an octameric structure, the extent of magnesium substitution within a particular site is limited, presumably because if the level of magnesium is too high, the oxo-cluster loses its structural integrity and dissociates. This was seen in the increasingly substituted complexes **21** and **22**, which were not found to have the structure and properties found in **19** and **20**.

It would be reasonable to expect there to exist a distribution of Zn : Mg contents throughout both crystalline materials **19** and **20**. However, our results indicate that the Zn : Mg content of each of these complexes was uniform and did not have an appreciable distribution. Slight changes in the starting ratios of Zn : Mg resulted in products with completely different solubility, volatility, and crystal structure properties (**19** and **20**). It is most likely this structural equilibrium excluded significant distributions in

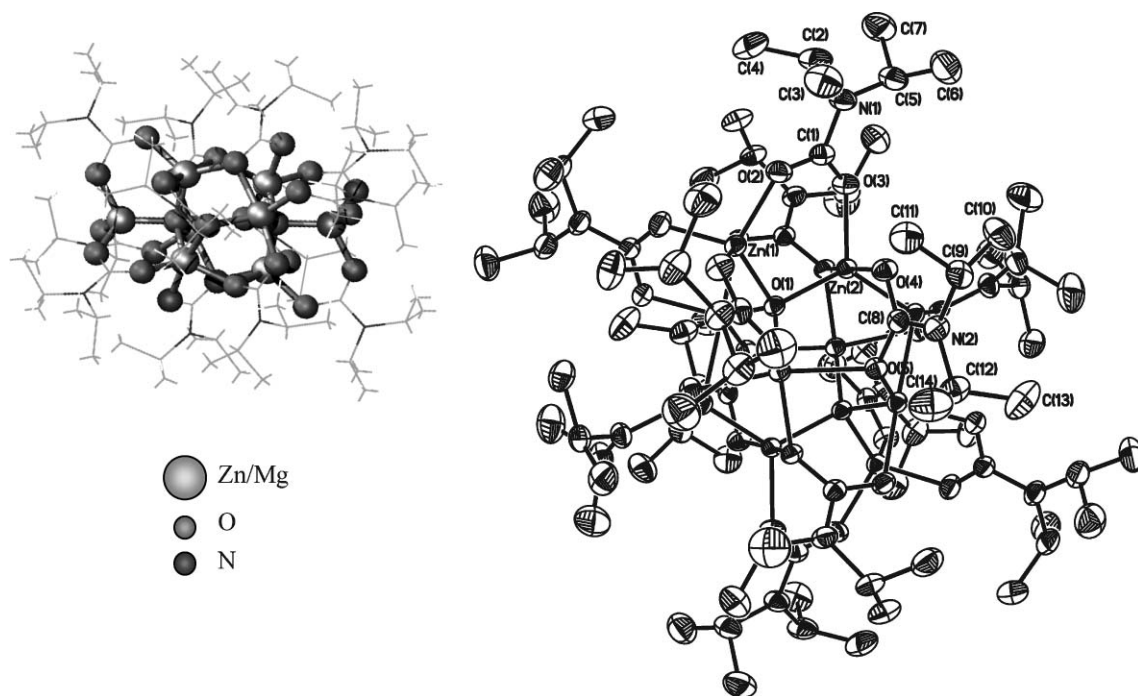


Fig. 3 Graphical representations of **20** as determined by X-ray crystallography.† Hydrogen atoms and heptane solvent molecules have been omitted for clarity. Thermal ellipsoids are drawn at the 50% probability level.

composition, as the octameric (**20**) and tetrameric (**19**) nuclearities appear to exist only for discrete starting Zn : Mg ratios.

Thermogravimetric analysis (TGA) demonstrates the promising nature of these complexes for SSCVD applications. In general, the spectra indicate a clean decomposition process at temperatures desirable to the SSCVD process. Along with the high volatilities observed in vacuum sublimation testing (Table 1), it is clear that these materials may be highly suited for use as SSCVD precursors.³² The volatile complexes **19** and **20** exhibit small but significant deviations in TGA from the pure zinc complex **7**. Whilst the primary mode of thermal decomposition commences at similar temperatures, the process is much quicker in the magnesium substituted analogues **19** and **20**, being completed ~50 and 100 °C lower respectively. It would be expected that the residues at the end of the decomposition process would be slightly lower for magnesium-substituted derivatives due to the lower atomic mass, but the minimally substituted complex **19** has a slightly higher percentage-weight residue. The small level of magnesium doping would be expected to cause a slightly lower percentage-weight residue than **7**, but the small difference (1–2%) is most likely within the instrumental limits. The residue of the more highly substituted **20** shows a pronounced difference, being ~7% lower than the pure zinc analogue **7**, and is indicative of the presence of the lower-atomic-mass magnesium atoms. The spectra help to explain the involatility of the high-magnesium-content complex **21** where there is a clear weight loss concomitant with heating (Fig. 4). The high levels of magnesium may compromise the stability of the metal oxide core of the complex. Presumably it is less stable because the octameric structure is compromised by the excess of magnesium within it.

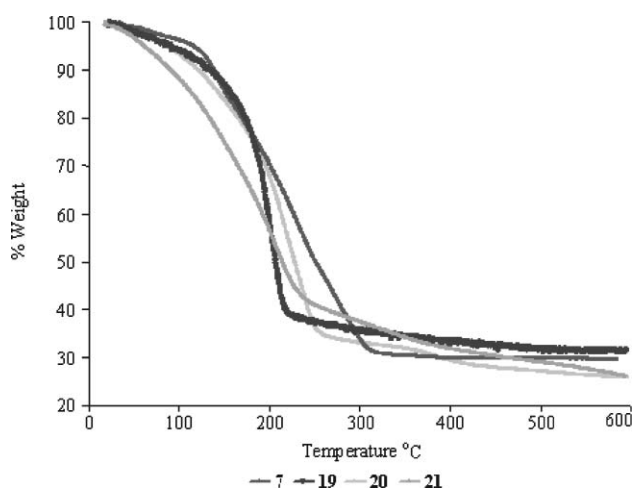


Fig. 4 Thermogravimetric analyses of Zn–Mg complexes **19–22** vs. pure zinc complex **7**.

Experimental

All manipulations were performed using standard Schlenk techniques. Infrared spectra were recorded as KBr disks and as neat liquids on a Perkin-Elmer 580B spectrometer. ¹H NMR and ¹³C NMR spectra were recorded on a Bruker AC300F spectrometer at 300 MHz. ¹H NMR data are reported as follows: chemical shift measured in parts per million (ppm) downfield from TMS (δ),

multiplicity, proton count, assignment. Multiplicities are reported as singlet (s), broad singlet (br s), doublet (d), triplet (t), quartet (q), sextuplet, septet and multiplet (m). ¹³C NMR shifts are reported in ppm downfield from TMS and identifiable carbons described. Microanalyses were performed in the microanalysis unit of the University of Otago, New Zealand. Solvents and reagents were purified by literature methods. Mass spectra of metal carbamate complexes could not be obtained due to their instability under ionisation. Meaningful data were not observed even with the most facile ionisation techniques, including electrospray and matrix-assisted laser desorption–ionisation (MALDI).

Zn_{4-x}Mg_x(μ_4 -O)(O₂CNⁱPr₂)₆ (**19**)

ZnEt₂ (2.89×10^{-2} mol) and ⁱPr₂NH (5.78×10^{-2} mol) in benzene (70 mL) were refluxed under a nitrogen atmosphere for 3 h to prepare 'EtZnNⁱPr₂'. To this mixture, a yellow solution of freshly prepared ⁿBuMgNⁱPr₂ (0.75 g, 4.125×10^{-3} mol) in THF (20 mL) was added. The reaction mixture was then exposed to CO₂ overnight, followed by the addition of H₂O (74.3 μ L, 4.13×10^{-3} mol) in THF (20 mL). As the water was added, the yellow colour of the solution was noticeably diminished. At the completion of reaction, the off-white powder was washed with MeCN (3 \times 50 mL) to remove some residual yellow unreacted magnesium moieties, leaving a white powder. The product was recrystallised from MeCN to afford a white powder **19** (5.21 g). ¹H NMR: (CDCl₃) δ (ppm): 1.02, (d, 12H, 4 \times CH₃CH), 1.16, (d, 60H, 20 \times CH₃CH), 2.90, (septet, 2H, 2 \times CH₃CH), 3.91 (septet, 10H, 10 \times CH₃CH). ¹³C NMR (CDCl₃) δ (ppm): 20.80, (CHCH₃), 23.34, (CHCH₃), 45.12, (CHCH₃), 45.63, (CHCH₃), 162.03, (CO₂). Calc. for Zn_{3.5}Mg_{0.5}O(O₂CNⁱPr₂)₆: Zn: 20.41, Mg: 1.07, C: 44.94, N: 7.49, H: 7.55. Found Zn: 20.30, Mg: 0.21, C: 47.50, H: 8.11, N: 7.88.

Zn_{7.38}Mg_{0.62}(μ_4 -O)₂(O₂CNⁱPr₂)₁₂ (**20**)

20 was prepared in a manner similar to that for **19**, using benzene (100 mL), ZnEt₂ (2.57 mL, 2.48×10^{-2} mol), ⁱPr₂NH (6.88 mL, 4.96×10^{-2} mol), ⁿBuMgNⁱPr₂ (1.50 g, 8.25×10^{-3} mol), CO₂ and H₂O (74.8 μ L, 4.15×10^{-3} mol) in THF (20 mL). A yield of 5.32 g of colourless crystals was recovered following crystallisation from hot heptane. ¹H NMR: (CDCl₃) δ (ppm): 1.05, (d, 24H, 8 \times CH₃CH), 1.15, (d, 24H, 8 \times CH₃CH), 2.90, (septet, 2H, 2 \times CH₃CH), 3.91 (septet, 2H, 2 \times CH₃CH). ¹³C NMR (CDCl₃) δ (ppm): 20.80, (CHCH₃), 23.32, (CHCH₃), 45.12, (CHCH₃), 45.63, (CHCH₃), 162.04, (CO₂). Calc. for Zn₇MgO₂(O₂CNⁱPr₂)₁₂: Zn: 20.41, Mg: 1.07, C: 44.94, N: 7.49, H: 7.55. Found Zn: 18.05, Mg: 0.40, C: 48.91, H: 8.50, N: 6.29.

5 EtZn(NⁱPr₂) + 3 BuMg(NⁱPr₂) + CO₂ + H₂O (**21**)

In a manner similar to that used for **19**, using benzene (100 mL), ZnEt₂ (2.25 mL, 2.07×10^{-2} mol), ⁱPr₂NH (5.73 mL, 4.13×10^{-2} mol), ⁿBuMgNⁱPr₂ (2.25 g, 1.38×10^{-2} mol), CO₂ and H₂O (74.8 μ L, 4.15×10^{-3} mol) in THF (20 mL). In this case, the solution washed from the white powder was a dark orange as opposed to the pale yellow observed in complexes **19** and **20** to deliver **21**. ¹H NMR: (CDCl₃) δ (ppm): 1.04–1.16, (d, septet, 70H, CH₃CH, CH₃CH), 2.90, (septet, 2H, 2 \times CH₃CH). ¹³C NMR (CDCl₃) δ (ppm): 20.75, (CHCH₃), 23.39, (CHCH₃), 45.12,

(CHCH₃) 45.71, (CHCH₃) 161.63, (CO₂). Because recrystallisation was not possible, a percentage yield could not be recorded.

4 EtZn(NⁱPr₂) + 4 BuMg(NⁱPr₂) + CO₂ + H₂O (22)

In a manner similar to that used for **19**, using benzene (100 mL), ZnEt₂ (1.87 mL, 1.80 × 10⁻² mol), ⁱPr₂NH (6.13 mL, 3.60 × 10⁻² mol), ⁿBuMgNⁱPr₂ (3.25 g, 1.80 × 10⁻² mol), CO₂ and H₂O (81.0 μL, 4.5 × 10⁻³ mol) in THF (20 mL), a white powder **22** was isolated. ¹H NMR: (CDCl₃) δ(ppm): 1.02, (d, 12H, 4 × CH₃CH), 1.16, (d, 6H, 2 × CH₃CH), 2.92, (septet, 2H, 2 × CH₃CH), 3.91 (septet, 1H, CH₃CH). ¹³C NMR (CDCl₃) δ(ppm): 20.80, (CHCH₃), 23.33, (CHCH₃), 45.11, (CHCH₃), 162.02, (CO₂). Because recrystallisation was not possible, a percentage yield could not be recorded.

X-Ray crystallography†

Single-crystal X-ray diffraction data for **19** and **20** were collected† at 150 K using a Bruker CCD-1000 area detector diffractometer employing graphite-monochromated Mo K α radiation. A full analysis was performed on one crystal in each case, and the cell volume was measured for several other crystals in each crop and found to be identical in each case. Data integration and reduction were undertaken with SAINT and XPREP,³³ and subsequent computations were carried out with the X-Seed graphical user interface.³⁴ An empirical absorption correction for **19** was determined with SADABS.³⁵ A Gaussian absorption correction³⁶ was applied to the data for **20**. Both structures were solved by direct methods with SHELXS-97³⁷ and extended and refined with SHELXL-97.³⁷

For **19**, all non-hydrogen atoms were modelled with anisotropic displacement parameters. Two of the ⁱPr₂NCO₂⁻ ligands (one on each unique complex) were each refined with disorder over two positions with occupancies of 0.67:0.33 and 0.72:0.28 respectively. Atoms occupying the same, or almost the same, sites were constrained to have the same anisotropic displacement parameters. Rigid bond restraints were applied to the thermal parameters of disordered atoms. A riding-atom model with group displacement parameters was used for all hydrogen atoms in the structure.

For **20**, all non-hydrogen atom sites in the Zn–Mg oxo-cluster were modelled with anisotropic displacement parameters, while those of the disordered heptane were modelled with isotropic displacement parameters. Zn and Mg atoms occupying the same position were constrained to have the same coordinates and anisotropic displacement parameters. The Zn–Mg occupancies were refined as free variables summing to unity for each of the two unique metal sites. Three general positions were identified for disordered heptane molecules having overlaps at the regions of maximum residual electron density as shown by difference maps for the cluster-only model. These three general positions were determined to have total unique occupancies of 0.25, 0.333333, and 0.166667 by examination of the 3D network of channels. The first was refined with one unique position (0.25), while the second and third were each refined with two separate positions at 0.208333/0.125 and 0.083333/0.083333 occupancies respectively. All heptane molecules were refined with 1–2 and 1–3 bond-distance restraints. Additionally, all carbon atoms within a given

heptane were constrained to have the same isotropic displacement parameters. A riding-atom model with group displacement parameters was used for all hydrogen atoms in the structure.

Summary and Conclusions

A novel strategy of mixing zinc and magnesium alkylamido intermediates has delivered the first reported Zn–Mg carbamate oligomeric complexes, which have been structurally characterised. By varying the starting Zn:Mg ratio, different structures were obtained according to the shifting of a fragile equilibrium between tetrameric and octameric nuclearities. The presence of magnesium was found to shift the equilibrium towards favouring the octameric structure seen in **20** due to its higher-coordination-number sites being more amenable to the incorporation of magnesium atoms. Confirmation of a successful reaction was shown with an array of experimental observations and characterisation techniques where significant variations from the related homometallic derivatives were found. In particular, refinement of the metal occupancies within **20** revealed 7.8% displacement of zinc by magnesium. The physicochemical properties of the synthesised precursor series were found to change significantly with the level of magnesium doping, largely as a result of the relative stabilities of the μ_4 -oxo cores with ranging magnesium substitutions. Complexes **19** and **20** were found to be highly volatile through vacuum sublimation tests at 5 × 10⁻⁶ Torr, and decomposed in a clean manner according to the TGA traces measured. Along with the relative ease of their synthesis, this indicated that they would be likely to be suitable for use as SSCVD precursors. The heterobimetallic oxo-bridged cluster complexes **19** and **20** are the first reported single-source Zn_xMg_{1-x}O precursors. Investigations into the films derived from these materials are ongoing.

Notes and references

- 1 F. O. Adurođija, in *Handbook of Thin Film Materials*, ed. H. Nalwa, Academic Press, Oxford, UK, 2001, vol. 1, pp. 161–217.
- 2 A. O. Dmitrienko, S. L. Shmakov, S. A. Bukesov and T. I. Goryainova, *Zh. Neorg. Khim.*, 1991, **36**, 480–484.
- 3 J. A. Sans and A. Segura, *High Pressure Res.*, 2004, **24**, 119–127.
- 4 Y. Segawa, *Oyo Butsuri*, 1998, **67**, 1295–1298.
- 5 X.-J. Zhang, H.-L. Ma, Q.-P. Wang, M. Jin, F.-J. Zong, H.-D. Xiao and J. Feng, *Wuli Xuebao*, 2005, **54**, 4309–4312.
- 6 Y. Zhang, J. He, Z. Ye, L. Zou, J. Huang, L. Zhu and B. Zhao, *Thin Solid Films*, 2004, **458**, 161–164.
- 7 G.-J. Fang, D. Li and X. Zhao, *Phys. Status Solidi A*, 2003, **200**, 361–368.
- 8 X. Zhang, X. M. Li, T. L. Chen, C. Y. Zhang and W. D. Yu, *Appl. Phys. Lett.*, 2005, **87**, 2101–2103.
- 9 E. Y. M. Lee, N. H. Tran, J. J. Russell and R. N. Lamb, *J. Phys. Chem. B*, 2003, **107**, 5208–5211.
- 10 A. J. Petrella, H. Deng, N. K. Roberts and R. N. Lamb, *Chem. Mater.*, 2002, **14**, 4339–4342.
- 11 M. R. Hill, A. W. Jones, J. J. Russell, N. K. Roberts and R. N. Lamb, *J. Mater. Chem.*, 2004, **14**, 3198–3202.
- 12 M. R. Hill, E. Y. M. Lee, J. J. Russell, Y. Wang and R. N. Lamb, *J. Phys. Chem. B*, 2006, **110**, 9236–9240.
- 13 A. Bacchi, D. B. Dell'Amico, F. Calderazzo, U. Giurlani, G. Pelizzi and L. Rocchi, *Gazz. Chim. Ital.*, 1992, **122**, 429.
- 14 M. T. Caudle, C. K. Mobley, L. M. Bafaro, R. LoBrutto, G. T. Yee and T. L. Groy, *Inorg. Chem.*, 2004, **43**, 506–514.
- 15 M. T. Caudle, J. B. Benedict, C. K. Mobley, N. A. Straessler and T. L. Groy, *Inorg. Chem.*, 2002, **41**, 3183–3190.
- 16 D. B. Dell'Amico, F. Calderazzo, L. Labella and F. Marchetti, *Inorg. Chim. Acta*, 2003, **350**, 661–664.

- 17 A. Belforte, F. Calderazzo, U. Englert and J. Strahle, *Inorg. Chem.*, 1991, **30**, 3778–3781.
- 18 C. S. McCowan, T. L. Groy and M. T. Caudle, *Inorg. Chem.*, 2002, **41**, 1120–1127.
- 19 D. B. Dell'Amico, F. Calderazzo, S. Farnocchi, L. Labella and F. Marchetti, *Inorg. Chem. Commun.*, 2002, **5**, 848–852.
- 20 U. P. Kreher, A. E. Rosamilia, C. L. Raston, J. L. Scott and C. R. Strauss, *Molecules*, 2004, **9**, 387–393.
- 21 P. F. Haywood, M. R. Hill, J. J. Russell, N. K. Roberts and R. N. Lamb, *Eur. J. Inorg. Chem.*, 2007, in press.
- 22 D. B. Dell'Amico, F. Calderazzo, L. Labella, F. Marchetti and G. Pampaloni, *Inorg. Chem. Commun.*, 2002, **5**, 733–745.
- 23 D. B. Dell'Amico, C. Bradicich, F. Calderazzo, A. Guarini, L. Labella, F. Marchetti and A. Tomei, *Inorg. Chem.*, 2002, **41**, 2814–2816.
- 24 D. B. Dell'Amico, F. Calderazzo, L. Labella, C. Maichlemosmer and J. Strahle, *J. Chem. Soc., Chem. Commun.*, 1994, 1555–1556.
- 25 K.-C. Yang, C.-C. Chang, C.-S. Yeh, G.-H. Lee and S.-M. Peng, *Organometallics*, 2001, **20**, 126–137.
- 26 M. T. Caudle, R. A. Nieman and V. G. Young, Jr., *Inorg. Chem.*, 2001, **40**, 1571–1575.
- 27 D. B. Dell'Amico, F. Calderazzo, L. Labella, F. Marchetti, M. Martini and I. Mazzoncini, *C. R. Chim.*, 2004, **7**, 877–884.
- 28 Y. Tang, L. N. Zakharov, A. L. Rheingold and R. A. Kemp, *Organometallics*, 2004, **23**, 4788–4791.
- 29 M. Ruben, D. Walther, R. Knake, H. Gørls and R. Beckert, *Eur. J. Inorg. Chem.*, 2000, 1055–1060.
- 30 E. C. Ashby and W. E. Becker, *J. Am. Chem. Soc.*, 1963, **85**, 118–119.
- 31 L. J. Guggenberger and R. E. Rundle, *J. Am. Chem. Soc.*, 1968, **90**, 5375–5378.
- 32 M. R. Hill, J. J. Russell and N. R. Lamb, *Chem. Mater.*, 2008, **20**, 2461–2467.
- 33 Bruker, *SMART, SAINT and XPREP. Area, detector control and data integration and reduction software. Bruker Analytical X-ray Instruments Inc.*, Madison, Wisconsin, USA, 1995.
- 34 L. J. Barbour, *J. Supramol. Chem.*, 2001, **1**, 189.
- 35 G. M. Sheldrick, *SADABS. Empirical, absorption correction program for area detector data.* University of Göttingen, Germany, 1996.
- 36 P. Coppens, L. Leiserowitz and D. Rabinovich, *Acta Crystallogr.*, 1965, **18**, 1035–1038.
- 37 G. M. Sheldrick, *SHELX97, Programs for crystal structure analysis.* University of Göttingen, Germany, 1998.